

# An *in situ* hydrogel based on carboxymethyl chitosan and sodium alginate dialdehyde for corneal wound healing after alkali burn

Wenhua Xu,<sup>1</sup> Kaibin Liu,<sup>2</sup> Tong Li,<sup>1,3</sup> Wenhua Zhang,<sup>1</sup> Yanhan Dong,<sup>5</sup> Jiayi Lv,<sup>1</sup> Wenli Wang,<sup>4</sup> Jingguo Sun,<sup>1</sup> Mengjie Li,<sup>1</sup> Meng Wang,<sup>1</sup> Zihong Zhao,<sup>1</sup> Ye Liang<sup>3</sup>

<sup>1</sup>Department of Inspection, The medical faculty of Qingdao University, Qingdao, 266003, China

<sup>2</sup>The Second Military Medical University, Shanghai, 200433, China

<sup>3</sup>Key Laboratory, Department of Urology and Andrology, The Affiliated Hospital of Qingdao University, Qingdao, 266003, China

<sup>4</sup>State Key Laboratory of Bioactive Seaweed Substances, Qingdao Bright Moon Group Co Ltd, Qingdao, 266555, China

<sup>5</sup>Institute for Translational Medicine, Qingdao University, Qingdao, 266003, China

Received 10 October 2018; revised 12 November 2018; accepted 5 December 2018

Published online 26 December 2018 in Wiley Online Library (wileyonlinelibrary.com). DOI: 10.1002/jbm.a.36589

**Abstract:** There is currently no optimal scaffold for the transplantation of limbal stem cells (LSCs) to induce corneal reconstruction after corneal alkali burns. This study attempts to fabricate a novel *in situ* Alginate-Chitosan hydrogel (ACH) for LSCs transplantation. Sodium alginate dialdehyde (SAD), a biological crosslinker, was prepared by periodate-mediated sodium alginate oxidization. Carboxymethyl chitosan was rapidly crosslinked with SAD *via* Schiff's base formation between the available aldehyde and amino groups. The ACH is rapidly formed on the wound surface by self-crosslinking without adding any chemical crosslinking component. Gelation time, transmittance, microscopic structure, equilibrium swelling, cytotoxicity, histocompatibility and degradability of the hydrogel were all examined. Rabbit primary LSCs were encapsulated in the hydrogel and transplanted to alkali burn wounds *in vivo*. Cornea reconstruction was evaluated by visual observation,

slit lamp, histological analysis, and immunofluorescence staining. Results showed that the *in situ* hydrogel was highly transparent, gelled quickly, biocompatible, and had low cytotoxicity. LSCs cultured *in vitro* expressed the stem marker p63 but lacked the differentiated epithelial markers cytokeratin 3 and 12. Furthermore, the hydrogel encapsulating LSCs could be formed quickly on the alkali burn wound of the cornea and was shown to significantly improve epithelial reconstruction. Taken together, treatment with this novel *in situ* hydrogel-mediated LSC transplantation system may serve as a rapid and effective method for corneal wound healing. © 2018 The Authors. *Journal of Biomedical Materials Research Part A* published by Wiley Periodicals, Inc. *J Biomed Mater Res Part A*: 107A: 742–754, 2019.

**Key Words:** carboxymethyl chitosan, limbal stem cells, sodium alginate dialdehyde, self-crosslinking, corneal wound healing

**How to cite this article:** Xu W, Liu K, Li T, Zhang W, Dong Y, Lv J, Wang W, Sun J, Li M, Wang M, Zhao Z, Liang Y. 2019. An *in situ* hydrogel based on carboxymethyl chitosan and sodium alginate dialdehyde for corneal wound healing after alkali burn. *J Biomed Mater Res Part A* 2019;107A:742–754.

## INTRODUCTION

Corneal alkali burn is one of the most serious ocular trauma, which could cause extensive corneal epithelia deficiency. During corneal wound healing, limbal stem cells (LSCs), an important source of corneal epithelial cells, rapidly migrate to the center of the cornea and cover the wound to form new epithelia. However, if LSCs are damaged and absent cornea reconstruction will be delayed, resulting in serious inflammation responses. The polymorphonuclear leukocytes release large amounts of proteases that degrade extracellular matrix components, leading to corneal ulcers,<sup>1</sup> opacification, and eventually loss of vision.<sup>2</sup> Thus, corneal wound healing

is critical for maintaining corneal transparency and recovering the eyesight.<sup>3</sup>

At present, corneal alkali burn is mainly treated by surgical intervention, such as corneal transplantation or amniotic membrane transplantation.<sup>1</sup> But corneal transplantation is easily lead to donor deficiency and immune rejection; although the amniotic membrane has similar horn and conjunctival components (type IV collagen fibers) in severe corneal alkali. However, this approach is associated with a series of adverse reactions,<sup>4</sup> including infection, immune rejection, and autopepsia.<sup>5</sup> Therefore, the treatment of corneal alkali burn must start from two aspects, one is to

**Correspondence to:** Y. Liang; e-mail: liangye82812@163.com or W. Xu; e-mail: qd.wh@163.com

Contract grant sponsor: National Natural Science Foundation of China; contract grant number: 81401899 and 81770900

Contract grant sponsor: the China Postdoctoral Science Foundation; contract grant number: 2017M622144

Contract grant sponsor: the Key Research and Development Program of Shandong Province; contract grant number: 2014GHY115025 and 2018GSF118197

Contract grant sponsor: the Qingdao Postdoctoral Application Research Project

Contract grant sponsor: the Qingdao Science and Technology Plan fund; contract grant number: 16-6-2-28-NSH and 15-9-1-51-jch

provide seed cells for timely repair of corneal epithelium; the other is to prevent further transformation of corneal stromal cells into myofibroblasts in order to inhibit the formation of scar tissue. LSCs play an essential role during cell proliferation and differentiation in the cornea and promote corneal injury repair.<sup>6</sup> However, there have not been LSC-based artificial corneas for clinical application until now, which is largely because of lacking of the suitable scaffold for cell transplantation. Hence, optimization of the carrier materials in the cornea tissue engineering is very important.

Chitosan has been widely used as a drug delivery material in general therapy and tissue engineering because it is biocompatible and biodegradable.<sup>7,8</sup> Carboxymethyl chitosan (CMCTS) is one of the chitosan derivatives, which has been shown to have good solubility, biodegradability, biocompatibility, and preventing abdominal adhesions and fibration.<sup>9,10</sup> Sodium alginate (SA) has also used for cartilage tissue engineering and wound dressing.<sup>11–15</sup> Its biodegradability may be further enhanced after SA is oxidized to its dialdehyde derivative, sodium alginate dialdehyde (SAD).<sup>16–19</sup> Our previous studies found that SAD prepared in water phase without chemical crosslinkings could greatly improve the hydrogen biosafety and avoid the toxicity.<sup>20</sup>

In this study, we attempt to prepare an *in situ* hydrogel through aldehyde groups of SAD self-crosslinking with free amino groups of CMCTS without adding any chemical crosslinking components and then studied its function in LSCs transplantation for corneal wound healing after alkali burn. Importantly, the novel hydrogel, formed *in situ* on the wound, could be the most beneficial for the scaffold of LSCs encapsulating and transplanting, which would provide a potential therapeutic way for corneal epithelial reconstruction based on tissue engineering.

## MATERIALS AND METHODS

### Materials and reagents

Protocols for animal experiments were approved by the Institutional Animal Care Center and Use Committee and were performed in accordance with the Association for Research in Vision and Ophthalmology Statement for the use of Animals. Kunming mice were purchased from Qingdao Laboratory Animal Center (Qingdao, China). New Zealand rabbits were purchased from the Agriculture Science Research, Department of Shandong Province (Jinan, China). CMCTS (degree of deacetylation = 96.44%, 134 kDa) was prepared in our laboratory. SA (105 kDa, G/M = 0.85) was obtained from Qingdao Bright Moon Group Co. (Qingdao, China). L929 mouse fibroblast and A431 epidermoid carcinoma cell lines were provided by the Institute of Biochemistry and Cell Biology of the Chinese Academy of Sciences (Shanghai, China). Sodium periodate and 3-(4,5-dimethylthiazol-2-yl)-2,5-diphenyltetrazolium bromide (MTT) were purchased from Sigma-Aldrich (St. Louis, MO). Materials for cell culture including Dulbecco's modified Eagle medium (DMEM), DMEM/F12 culture medium, fetal bovine serum (FBS), trypsin, penicillin, and streptomycin were purchased from Gibco (Grand Island, NY).

### Synthesis of SAD

SAD was prepared by the periodate oxidation method.<sup>17</sup> Briefly, it was generated by oxidation of SA in an ethanol-water mixture (1:1) with sodium periodate as the oxidizing agent. The molar ratio of sodium periodate to alginate was 1:4. The suspension was maintained in the dark and stirred at room temperature for 6 h. The oxidized products were precipitated and rinsed with ethanol under stirring, then dried at room temperature under vacuum. All experiments were performed under sterile conditions. Aldehyde structures of SAD were analyzed by Fourier transform infrared spectroscopy (FTIR). The IR spectra of SA and SAD (~0.5 mg) were acquired with a Thermo Nicolet Nexus 470 spectrometer (Madison, WI) using KBr pellets at room temperature.

### Preparation of the composite hydrogel

CMCTS prepared in our laboratory has been characterized previously.<sup>21</sup> SA, SAD, and CMCTS were separately dissolved in 0.9% NaCl aqueous solution at a concentration of 20 mg/mL. Equivalent volumes of the two solutions, SAD and CMCTS, were then mixed at room temperature to form the crosslinked composite SAD-CMCTS hydrogel (SC), comparing with the mixture of SA and CMCTS.

### Hydrogel characterization

**Transparency.** The SC was added to a 96-well plate (100  $\mu$ L/well), and absorbance was measured at wavelengths of 400, 500, 600, 700, and 800 nm, respectively at room temperature with a Thermo Multiskan Go Spectrum spectrophotometer (Vantaa, Finland). Normal saline was used as a blank control.

**Microstructure.** SC samples were frozen overnight at  $-80^{\circ}\text{C}$  and then lyophilized for 24 h. The freeze-dried products were mounted on sample stubs and sputter-coated with gold, and images were acquired on a scanning VEGA3 electron microscope (Tescan, Brno, Czech Republic).

**Swelling capacity.** The swelling ratio (SR) of the SC was measured as previously described.<sup>22</sup> The SC was immersed in deionized water at room temperature for 2 days until equilibrium was reached in terms of swelling. After absorbing excess water on the surface with filter paper, the swollen SC was immediately weighed ( $W_s$ ). The SC was prefrozen overnight at  $-80^{\circ}\text{C}$ . After lyophilization for 24 h, the dry weight ( $W_r$ ) was determined. Measurements were performed in triplicate, and SR was calculated with the following formula:  $\text{SR} = (W_s - W_r)/W_r$ .

### Cytotoxicity studies

The cytotoxicity of SC was tested according to International Organization for Standardization standards (GB/T16886.5–2003) by culturing L929 mouse fibroblasts with SC extracts. The prepared SC was incubated in complete medium for 24 h at  $37^{\circ}\text{C}$ . A volume of saline solution equivalent to that of the SC was added to provide the control. L929 cells were cultured in DMEM supplemented with 10% FBS at  $37^{\circ}\text{C}$  and 5%  $\text{CO}_2$ . When they reached logarithmic growth, cells were collected and resuspended at a

density of  $4.0 \times 10^4$  cells/mL, added to 96-well plates at 200  $\mu$ L/well, and incubated overnight at 37°C and 5% CO<sub>2</sub>. The culture medium was replaced with gel extract for the experiment group. Cells cultured in medium alone served as the normal control and those cultured with extracts containing equal volumes of normal saline served as the solvent control. Each sample was prepared in triplicate. On the first, second, and third day, the MTT assay was performed by measuring optical density at 490 nm (OD<sub>490</sub>). The relative growth rate (RGR) was determined with the following formula:  $RGR (\%) = (OD_1 - OD_0) / (OD_2 - OD_0) \times 100\%$ , OD<sub>0</sub>, OD<sub>1</sub>, and OD<sub>2</sub> are the average ODs of the blank, experimental, and solvent control groups, respectively. The results were scored as 0 (nontoxic, RGR  $\geq$  100%), 1 (slightly cytotoxic, RGR = 75–99%), 2 (moderately cytotoxic, RGR = 50–74%), and 3 (severely cytotoxic, RGR = 25–49%). The experiment was performed three times.

### **In vivo degradation assay**

Kunming mice (weighing about 20 g, 6 weeks old, half males and half females) were housed under specific pathogen-free conditions. Sterile SC (100  $\mu$ L) was injected into the skeletal thigh muscle of anesthetized mice. Mice that received an equal injection of saline acted as the negative control group. After injection, three mice from each group were sacrificed each week for 4 weeks to assess hydrogel degradation. The muscle and tissues surrounding the injection site were removed, fixed in 10% neutral-buffered formaldehyde, and embedded in paraffin for conventional hematoxylin-eosin (HE) staining. After being weighed, the liver, kidney, and spleen were also collected, weighed, fixed, and HE-stained. The liver, kidney, and spleen index of the experimental animals were calculated using the following formula to analyze the toxicity of the hydrogel *in vivo*: Relative weight =  $W/W_0$ , where  $W$  was the weight of liver, kidney, or spleen, and  $W_0$  was the weight of experimental animals.

### **Cytocompatibility of SC with LSCs**

**Primary culture of LSCs.** LSCs were derived from the eyes of healthy New Zealand white rabbits (1 month old) as previously described.<sup>23</sup> Briefly, under a dissecting microscope, an incision was made in the conjunctival membrane 3 mm behind the limbus and carefully cut toward the limbus into the cornea up to 1 mm. After removing the conjunctival membrane, the limbal ring tissue was excised and cut into pieces of approximately 1–2 mm<sup>2</sup>. The corneal margin tissue was removed and corneal epithelia were dissected from the central portion. The epithelial layer was collected and dissociated for primary culture of corneal epithelial cells (CECs). The cells were cultured in DMEM/F12 medium containing 15% FBS using the tissue block method.<sup>23</sup> Isolated cells were incubated at 37°C and 5% CO<sub>2</sub> until use.

**LSC identification by western blotting.** After culturing primary LSCs for 5 days, cell lysates were harvested for western blotting.<sup>24</sup> Rabbit monoclonal anti-p63 antibody (Abcam, Cambridge, UK) and mouse monoclonal anti-glyceraldehyde 3-phosphate dehydrogenase (GAPDH) antibody (Novus Biological, Littleton, CO) were used as primary antibodies.

A chemiluminescence horseradish peroxidase substrate detection kit (Millipore, Bedford, MA) and Fluor Chem Q imaging system (Alpha Image, San Jose, CA) were used to visualize protein bands. Data were normalized to the level of GAPDH. A431 and CEC lysates were prepared as described above and used as positive and negative controls, respectively.

### **LSC identification by immunofluorescence analysis.**

Primary LSCs and CECs were cultured on glass slides for 5 days, then fixed with 4% paraformaldehyde for 10 min and rinsed twice with phosphate-buffered saline (PBS). Cells were incubated overnight at 4°C with antibodies against p63 or the CEC markers cytokeratin 3 and 12 (K3 + 12; Abcam). After three washes with PBS, the cells were incubated for 1 h at room temperature with Cy3- or FITC-conjugated secondary antibodies, washed three times with PBS, and stained with 4',6-diamidino-2-phenylindole (DAPI) for 10 min at room temperature to label cell nuclei. Samples were examined under a fluorescence IX73 microscope (Olympus, Tokyo, Japan). We captured five images for each group. DAPI could stain the nucleus of all the cells, which indicated the total amount of cells in each captured image. At the same time, the marker protein stained with fluorescent antibody indicated the positive cells. Image J software was used to help determining the average amount of DAPI (blue) in each field ( $N_d$ ) as well as the average amount of K3 + 12 in the same image ( $N_k$ ). The positive rate (PR) was calculated with the following formula:  $PR = N_k / N_d \times 100\%$ .

**Cytocompatibility.** The cytocompatibility of SC with LSCs was evaluated using the MTT assay and 5,6-carboxyfluorescein diacetate succinimidyl ester (CFSE) staining. SC extracts were prepared as described in Section 2.5. LSCs were seeded on a 96-well plate (200  $\mu$ L/well) at a density of  $6 \times 10^5$  cells/mL and incubated for 24 h at 37°C in a humidified atmosphere of 5% CO<sub>2</sub>. The cells were cultured with SC extracts, as described in Section 2.5, for 48 and 72 h, and then stained with CFSE. Cellular adhesion and viability were observed with a fluorescence microscope.

### **Application and evaluation of LSCs encapsulated in SC for alkali burn wound healing**

**Alkali burn model.** New Zealand white rabbits ( $n = 15$ , weighing approximately 2 kg, female) were randomly divided into normal ( $n = 3$ ), model ( $n = 6$ ), and experimental groups ( $n = 6$ ), and the left eyes were used for surgery. Prior to disease induction and treatments, rabbits were thoroughly examined for any corneal abnormalities. The animals were anesthetized *via* intravenous injection of 2% pentobarbital sodium solution (1 mL/kg) and then fixed on an operating table. The ocular surface was washed with 0.9% normal saline and the eyelids were disinfected with iodophor. After introducing one drop of topical 0.4% oxybuprocaine eye drop into the oculus sinister, sterile filter paper (round, 8 mm in diameter) that had been completely soaked in 1 M NaOH was placed on the center of the cornea for 30 s to create a well-circumscribed corneal burn wound. The burned ocular surface was promptly washed with a large volume of 0.9% saline solution. In the experimental group, sterile

2% CMCTS encapsulated with primary or P1 LSCs cultured *in vitro* was mixed with an equal volume of sterile 2% SAD. After 60 s, the *in situ* SC was formed on the burned ocular surface, and the upper and lower eyelids were sutured shut. The model group received no other treatment after the burn wound. Ofloxacin was applied dropwise to all operated eyes after surgery to prevent infection.

**General and slit lamp observation of wound healing status.** Stitches were removed 5 days after surgery. Changes to the ocular surface and wound healing status were photographed for each group on days of 0, 7, 14, 21, and 28. Corneal turbidity area<sup>21</sup> was measured using Image J software and calculated with the following formula: % turbid area =  $(S / S_0) \times 100\%$ , where  $S_0$  and  $S$  represent the corneal cloudy areas of experimental and model animals before and after repair, respectively. After 28 days, the ocular surface of each group was observed under a slit lamp (SL-2G; Topcon, Tokyo, Japan).

**Histological observation and fluorescence microscope imaging.** Animals were sacrificed on day 28 after surgery, and their corneas were removed and cut into two equal parts along the midline. One part was fixed in 10% neutral-buffered formaldehyde for HE staining, and the other was prepared as frozen sections for immunofluorescence analysis of K3 + 12 and stroma cell marker vimentin (Bioss, Beijing, China) expression. The sections were examined by fluorescence microscopy.

#### Statistical analysis

Data are shown as mean  $\pm$  standard deviation (SD) of duplicate or triple experiments and were analyzed using SPSS v.19.0 software (SPSS Inc., Chicago, IL). Mean differences were evaluated by one-way analysis of variance or with the *t*-test, and  $p < 0.05$  was considered statistically significant.

## RESULTS

### SC gelation by self-crosslinking and microstructure observation

The physicochemical properties of SA are listed in Table I. SA from a standard range of GB1886 243-2016 was used to prepare SAD. Changes to the structure of SA and SAD were confirmed by FTIR spectroscopy. A new absorption peak at about  $1728.32 \text{ cm}^{-1}$  was detected in the spectrum of SAD [Fig. 1(A)], which corresponded to the  $\text{—C=O}$  bond of the aldehyde group. The gelation of SC was attributed to the Schiff base reaction between the  $\text{—CHO}$  groups of SAD and the  $\text{—NH}_2$  groups of CMCTS [Fig. 1(B)]. SAD and CMCTS could crosslink and form the SC obviously at room temperature after mixing for about 40–60 s, and SA and CMCTS could not form hydrogel at the same time [Fig. 1(C)]. Hydrogel microstructure is known to influence cell proliferation and adhesion. A morphological analysis by scanning electron microscopy revealed a highly porous SC, with pores of irregular shape and an interconnected inner structure [Fig. 1(D)]. The variable shape and texture of the hydrogel may provide a suitable scaffold for cell growth and nutrient permeability.

**TABLE I. Properties of sodium alginate**

Item	Standard	Test results
Moisture %	$\leq 15.0$	11.34
PH value	6.0~8.0	7.38
Insoluble matter in water %	$\leq 0.6$	0.51
Ash content %	18.0~27.0	24.27
Color and status	Light fawn powder	Light fawn powder
(Pb) (lead), mg/kg	$\leq 4.0$	<4.0
(As) (lead), mg/kg	$\leq 2.0$	<2.0

### Optical transmittance and swelling capacity

The optical transmittance of SC was determined at different wavelengths, ranging from 400 to 800 nm. As shown in Table II, optical transmittance of the hydrogel was above 77% at all wavelengths. In comparison, the optical transmittance of the human cornea ranges from 50 to 75% across various spectral regions.<sup>25</sup> These findings indicate that the SC hydrogel meets the standards for normal vision.

### Cytotoxicity of SC

Cytotoxicity experiments were carried using L929 mouse fibroblast cells cultured with SC extracts. Notably, culturing the cells with the SC hydrogel did not induce any cytotoxicity compared to the control group at any time point (Fig. 2). This was particularly apparent during our analysis of the RGR at 24, 48, and 72 h, which revealed no significant differences between normal saline and SC groups ( $p > 0.05$ ), indicating that the material had no obvious cytotoxicity. Furthermore, the morphology of L929 mouse fibroblasts cultured with gel extracts was also similar to that of normal saline and control cells at these time points. Cell morphology was consistent with the  $\text{OD}_{490}$  value obtained during RGR measurements. Cells were interconnected and there was no difference in morphology between groups. These results confirm that the SC hydrogel prepared in this study has no significant cytotoxic effect *in vitro*.

### Degradation of SC in vivo

The biodegradability of the SC hydrogel was assessed by implantation into the muscle of Kunming mice. All treated mice lived, and no obvious infection or distress was observed. Histologically, similar levels of inflammation were observed for both the control (injected with normal saline) and SC groups in the first week (Fig. 3). An inflammatory response appeared to occur in the SC groups after one week, possibly caused by gel degradation, however it subsided during weeks 2 and 3. By the fourth week, no inflammatory signals were observed in the treated animals [Fig. 3(A)]. These results suggest that the gel was completely degraded over the observation period, and the inflammatory response it induced was equivalent to that of saline.

Liver, kidney, and spleen tissues of the control and SC groups were also analyzed at the end of the observation period. Notably, no significant differences were observed between the tissues of control or SC hydrogel-treated groups

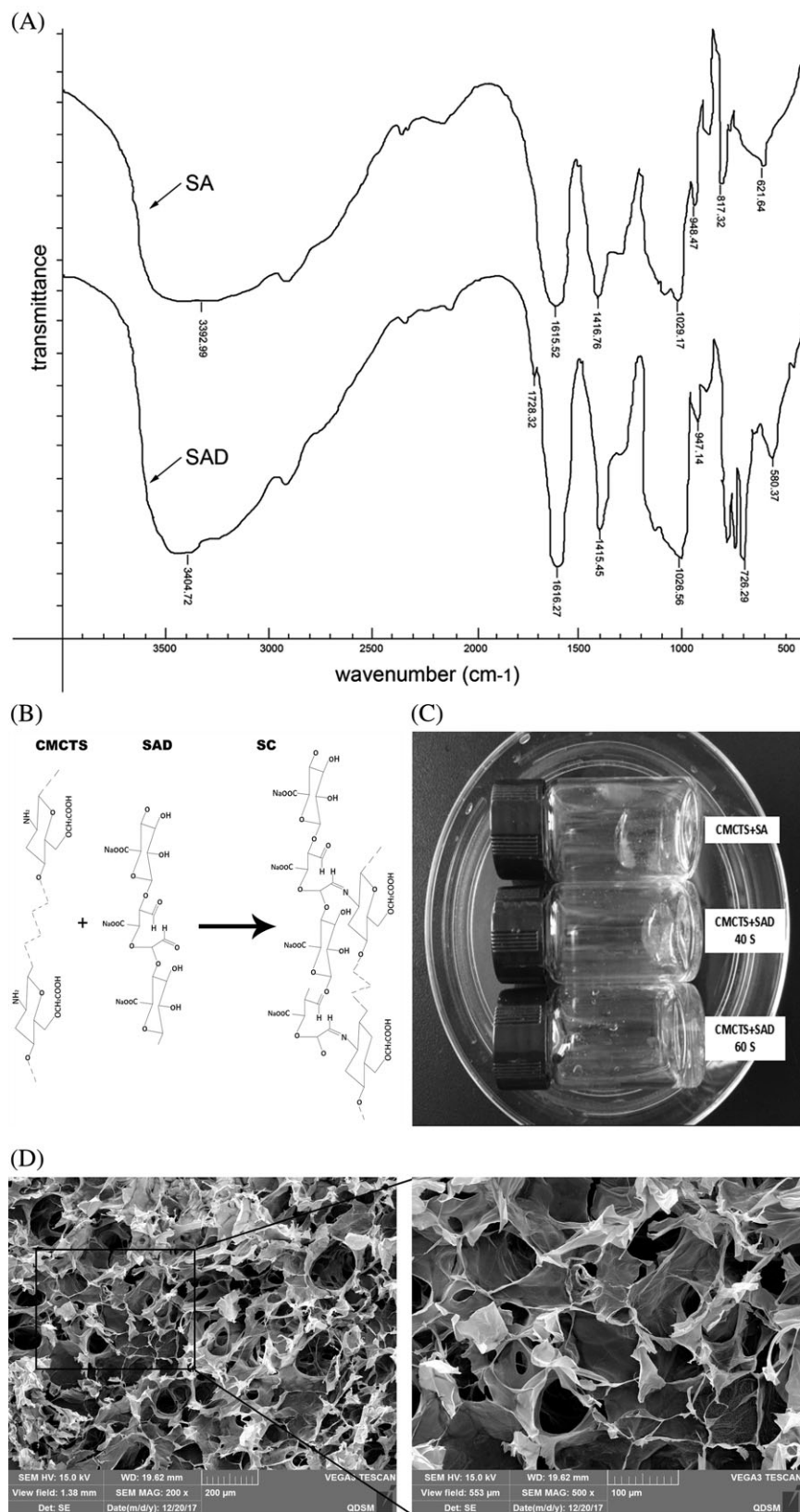


**FIGURE 1.** SC gelation and microstructure. (A) FTIR spectra of SA and SAD; (B) Chemical structure of SC following self-crosslinking of CMCTS with SAD; (C) The picture of the hydrogel formation; and (D) SC microstructure detected by scanning electron microscopy, highlighting numerous irregular pores.

**TABLE II. Optical transmittance of the SC**

Wavelength (nm)	Transmittance (% , mean $\pm$ SD)
400	77.78 $\pm$ 0.44
500	85.10 $\pm$ 0.24
600	87.44 $\pm$ 0.43
700	88.31 $\pm$ 0.20
800	88.11 $\pm$ 0.31

Data represent mean  $\pm$  SD of three experiments.

based on histological analysis [Fig. 3(B)] or tissue weight [Fig. 3(C),  $p > 0.05$ ].

### LSCs identification

As expected, p63 was highly expressed in A431 cells, whereas no expression could be detected in CECs following western blot analysis [Fig. 4(A)]. The presumptive LSCs cultured from different tissue blocks were labeled “a,” “b,” “c,” “d,” “e,” “f,” and “g.” Although all appeared to express p63,

there were some notable differences among the samples, with groups “c” and “g” exhibiting higher expression than other groups and thus being identified as LSCs. These LSCs and CECs were then stained with antibodies against K3+12 and DAPI and the positive rate was analyzed [Fig. 4(B)]. CECs highly expressed K3+12, whereas in LSCs expression was below 20% (\*\* $p < 0.01$ ). Moreover, immunostaining revealed significant p63 expression in both A431 cells and LSCs [Fig. 4(C)]. Statistical analysis indicated that p63 expression was similar in both cell types ( $p > 0.05$ ) and was positive in more than 90% of cases. These results suggest that K3+12 and p63 expression can be used to successfully identify LSCs.

### SC hydrogel cytocompatibility with LSCs in vitro

To evaluate SC hydrogel cytocompatibility with LSCs, proliferation of LSCs cultured with the gel extracts for 24, 48, and 72 h was assessed using the MTT assay. As shown in Figure 5(A), there was no statistically significant difference in cell proliferation between LSCs treated with SC extracts

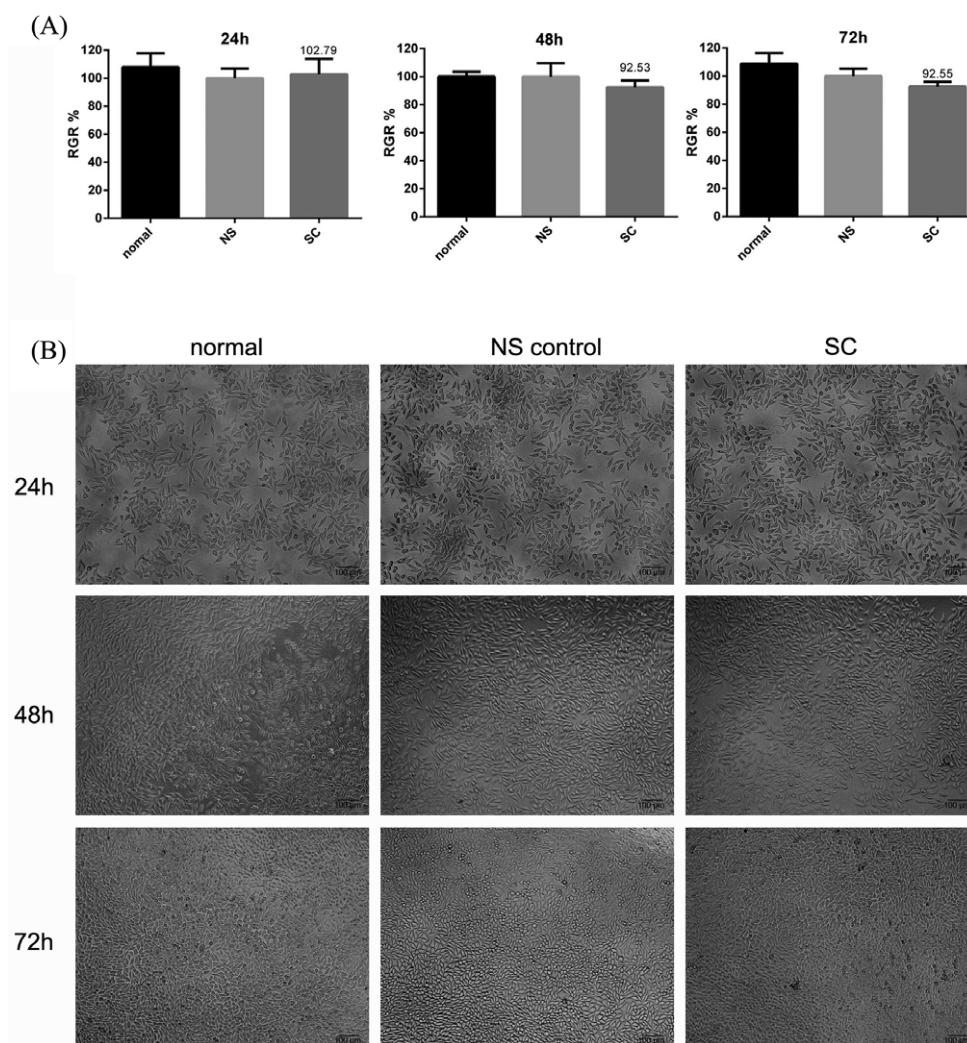


**FIGURE 2.** SC cytotoxicity in L929 mouse fibroblast cells cultured with SC extracts. RGRs (A) and cell morphology (B) were measured at 24, 48, and 72 h in untreated (normal), normal saline-treated (NS), and SC hydrogel-treated cells (SC). Scale bar = 100  $\mu$ m.

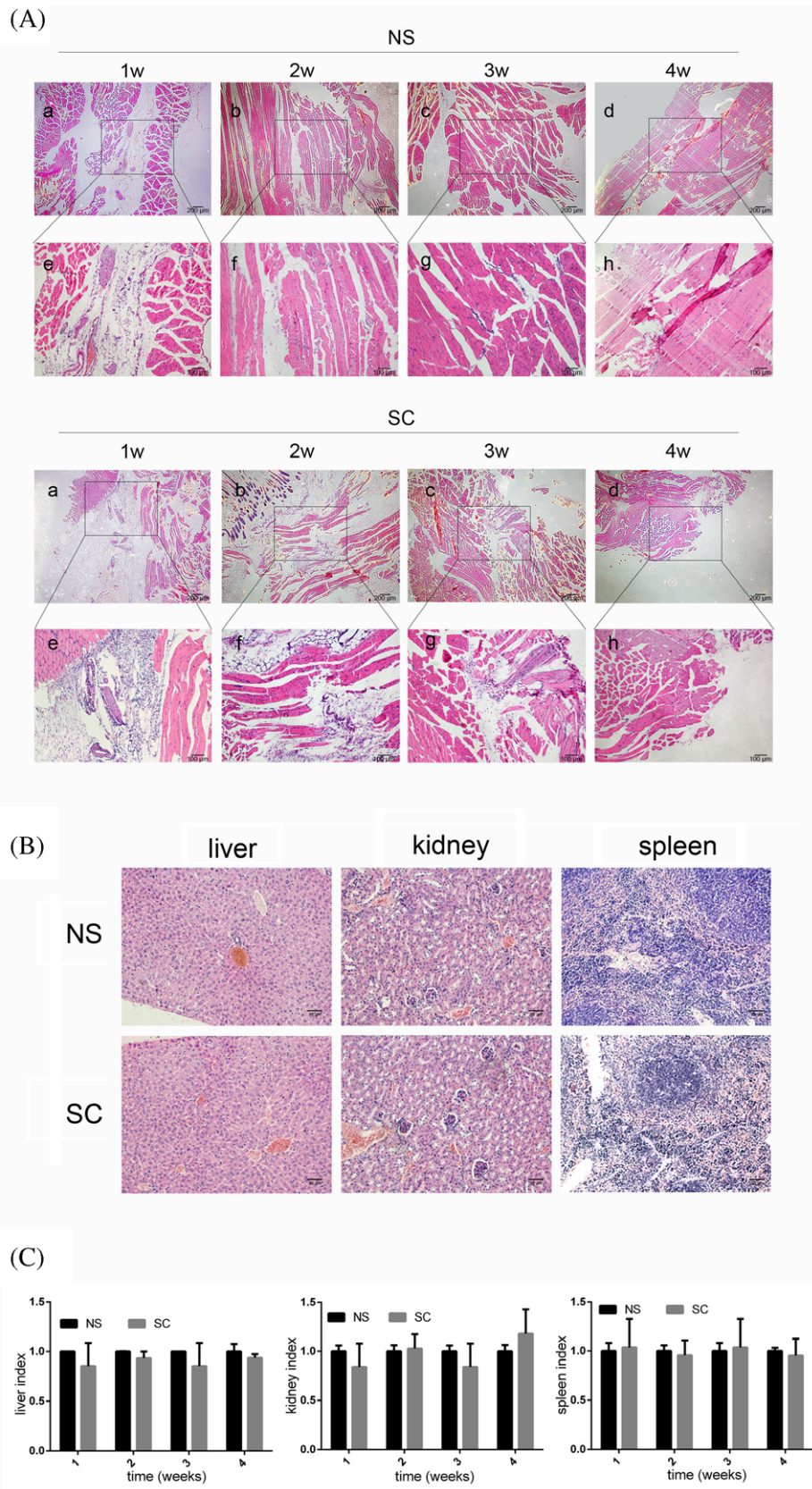


**FIGURE 3.** Histological analysis of hydrogel degradation and the inflammatory response over 4 weeks. (A) Representative images of HE-stained muscle tissues injected with either normal saline (NS) or SC hydrogel at each time point. Scale bars = 200  $\mu\text{m}$  (a-d), 100  $\mu\text{m}$  (e-h). (B) Histological analysis of liver, kidney, and spleen tissues by HE staining. Scale bars = 50  $\mu\text{m}$ . (C) Organ indices in SC and NS control groups.

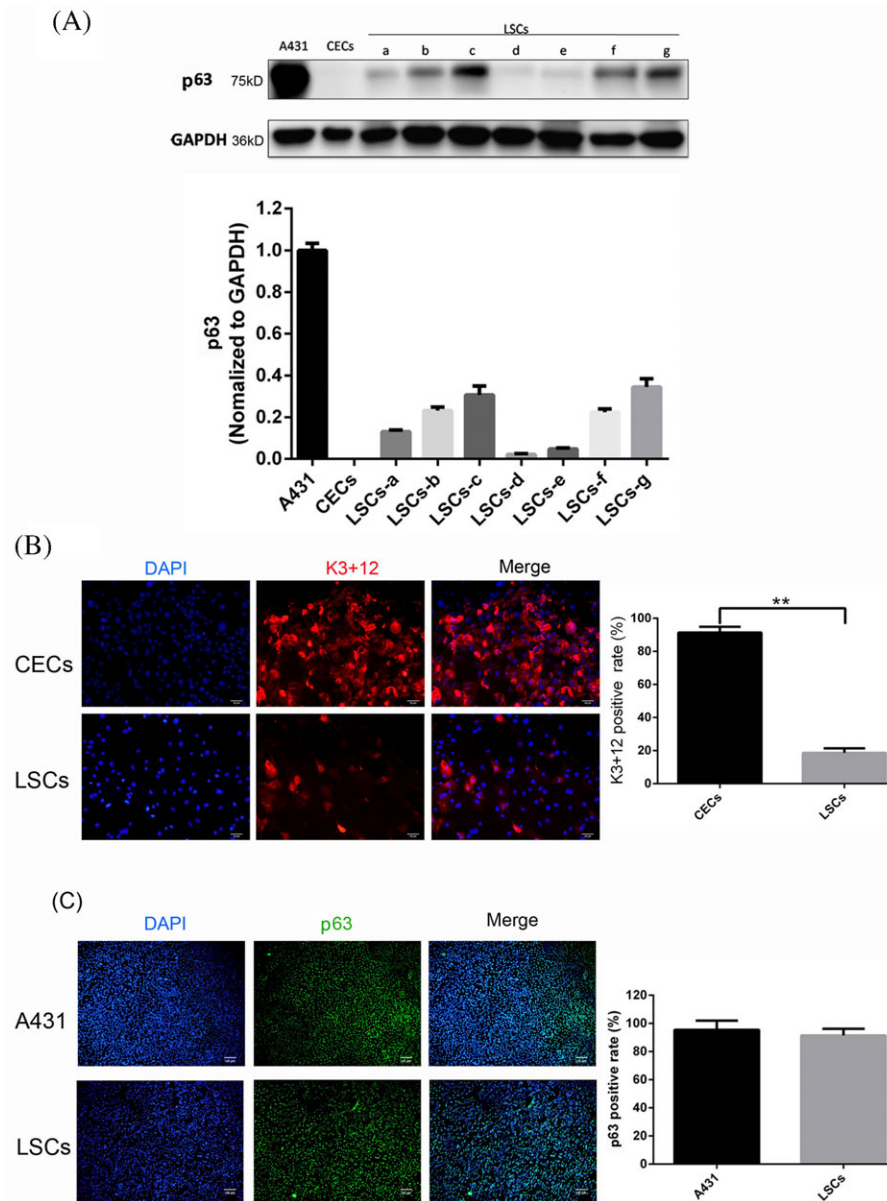


**FIGURE 4.** Identification of LSCs based on p63 and K3+12 expression. (A) Expression of p63 was quantified by western blotting. Protein expression was normalized to that of GAPDH. (B) Representative images of K3+12-stained CECs and LSCs, and the corresponding expression (right panel). Scale bars = 50  $\mu$ m. (C) Representative images of p63-stained A431 cells and LSCs, and the corresponding expression (right panel). Scale bars = 100  $\mu$ m. Data are presented as the mean  $\pm$  SD for each group from three experiments. \* $p$  < 0.05, \*\* $p$  < 0.01.

and control cells after 48 h ( $p > 0.05$ ), even though proliferation was slightly reduced in the SC group relative to the normal saline control at 72 h. Furthermore, cell adhesion and growth were also detected by CFSE staining at 48 and 72 h [Fig. 5(B)]. Compared with controls, LSCs maintained their normal morphology and reached almost complete confluence when cultured with SC extracts. These results suggest that the SC hydrogel is cytocompatible with LSCs.

#### Treatment of ocular alkaline burn wound by LSCs-encapsulating SC hydrogel

**General observation of wound healing status.** After surgery, we did not observe any corneal perforations or infection in any

of the rabbits in this experiment. Results showed that treatment of corneal alkali burns with our novel hydrogel reduced corneal opacity completely within 28 days' postburn [Fig. 6(A and B)]. After 7 days, an obvious reduction in corneal opacity was observed for the hydrogel-treated compared to the untreated model group. Moreover, after 14 days, corneal opacity was further decreased in the treated group. Neither the treated nor untreated model groups exhibited any ocular secretion at this stage. The treatment-induced decrease in opacity persisted at 21 days' postsurgery and by 28 days, and corneal transparency in the hydrogel-treated group was comparable to that in a normal cornea. At the same time, an obvious opacification could still be observed with the naked eye in the untreated group.

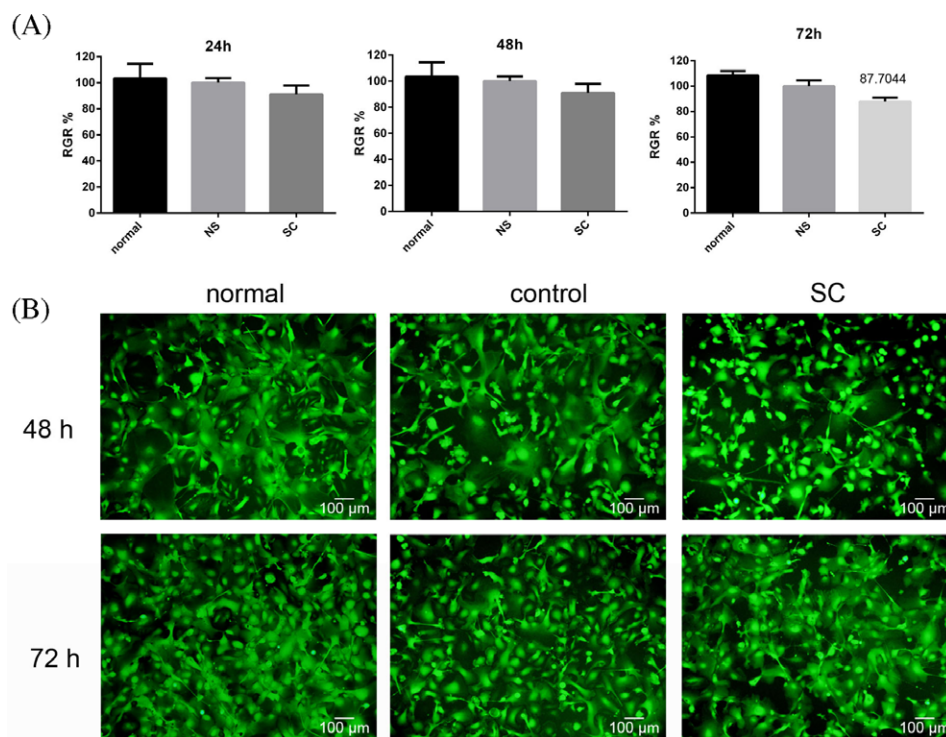


**FIGURE 5.** SC cytocompatibility in LSCs cultured with SC extracts. (A) RGR of LSCs at 24, 48, and 72 h. (B) Cell viability detected by CFSE staining at 48 and 72 h. Cells grown in medium alone or control extract solution (NS) served as the normal and solvent control groups, respectively, and cells cultured with SC extract constituted the experimental group. Scale bars = 100 μm.

These results were consistent with the slit lamp observation on day 28 [Fig. 6(B)]. In fact, compared to the untreated model group, the level of turbidity in the hydrogel-treated group was significantly lower at all time points [Fig. 6(C),  $p < 0.001$ ]. All these results indicate that the corneal injury caused by alkaline burn could be repaired by treatment with LSCs-encapsulating SC hydrogel.

**Histological analysis of the wounded cornea.** Although wound healing was observed with the naked eye, it was essential to evaluate these changes at a histological level. At day 28 postburn, an area characterized by clear epithelial defects was present in the model group, indicating that little self-healing of the structure had occurred [Fig. 7(A), middle panels]. However, these defects were largely healed in the hydrogel-treated group [Fig. 7(A), right panels], where the epithelial layer was similar to that observed in the normal, unburned cornea [Fig. 7(A), left panels]. Furthermore, although the epithelial layer of the treatment group appeared to be slightly thinner than that of the normal cornea and there was a statistically significant difference in the epithelial layer between the treatment and model groups [ $p < 0.05$ , Fig. 7(B)], no such difference in corneal thickness was detected between the normal and treatment groups [ $p > 0.05$ , Fig. 7(C)]. Instead, the thickness of the model cornea was significantly greater than that of both the normal and hydrogel-treated groups ( $p < 0.001$ ).

**Immunofluorescence analysis of wound healing status.** K3 +12 and vimentin were used, respectively, as epithelial and stromal markers for immunofluorescence analysis of wound healing after corneal alkali burn (Fig. 8). Notably, no significant differences were observed between the hydrogel-treated and normal unburned groups. Lack of any obvious expression of K3+12 in the model group indicated that few epithelial cells were present. These results are consistent with our previous observations (Figs. 6 and 7), all of which suggest that treatment of alkali burns using a combination of SC hydrogel and LSCs effectively promotes corneal injury repair.

## DISCUSSION

The cornea is a three-layered structure comprising the epithelial, stromal, and endothelial layers. The corneal epithelia are continually renewed by proliferating and differentiating. LSCs, located in the basal layer of the limbus, play an important role in maintaining a clear and healthy cornea and preserving vision.<sup>26</sup> LSCs grow inward toward the center of the cornea and gradually differentiate into corneal epithelia.<sup>27</sup> Furthermore, LSC deficiency and/or the loss of corneal epithelia have been shown to greatly affect vision.<sup>28</sup> Serious alkali burns, for example, have been shown to result in LSC deficiency, and the subsequent absence of epithelia ultimately leads to chronic inflammation, conjunctival in-growth, neovascularization, reduced vision, and blindness.<sup>29,30</sup> Therefore, to recover eyesight after an alkali burn, it is important to maintain the integrity of the epithelia. In the present study, we

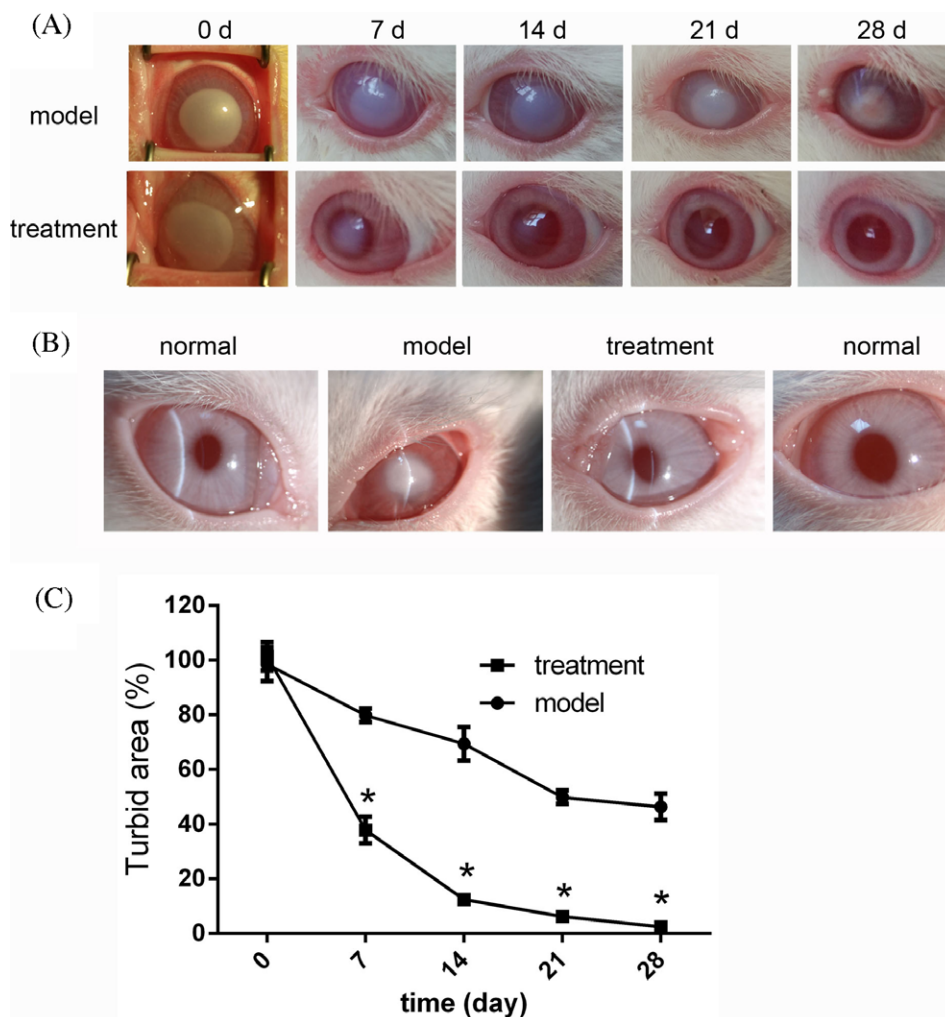


**FIGURE 6.** Treatment with LSC-encapsulating SC hydrogel induces a visible wound healing response in the cornea after alkali burn. (A) Representative images of untreated burn model (upper panels) and the hydrogel-treated group (lower panels) at 0, 7, 14, 21, and 28 days post-burn. (B) Representative slit lamp images of unburned (normal), untreated model, and hydrogel-treated rabbit corneas 28 days' postburn. (C) Statistical analysis of corneal turbidity 0, 7, 14, 21, and 28 days' postburn in the model and treatment groups (\* $p < 0.001$ ).

transplanted LSCs using an *in situ* self-crosslinking hydrogel in a rabbit corneal alkali burn model. The hydrogel was evaluated with its structural characteristics, biocompatibility, and degradation.

Liang et al.<sup>20</sup> previously transplanted corneal endothelia into a composite hydrogel made of self-crosslinking hydroxypropyl chitosan and SAD. In their analysis, corneal endothelia were successfully reconstructed using the *in situ* hydrogel. Furthermore, Huang et al.<sup>24</sup> previously applied a combination of dexamethasone and Avastin using a supramolecular hydrogel in a rat alkali burn model, which resulted in attenuation of inflammatory corneal neovascularization. Tsai et al.<sup>31</sup> utilized CTS-based hydrogel loaded with ferulic acid (FA) for corneal wound healing and showed that the FA-loaded hydrogel could promote wound healing. However, few studies have attempted to transplant LSCs and none has used the particular type of hydrogel to treat severe alkali burns.

The *in situ* hydrogel prepared in this study was derived from chitosan and SA. Chitosan is found in insects, fungi,

yeasts, and invertebrates.<sup>32</sup> The FDA has approved its wound healing and antibacterial effects as well as its biocompatibility. Furthermore, SA is a naturally polysaccharide that is stable, water soluble, viscous, and safe. Based on the properties and effects of the two components, a hydrogel prepared using both materials could have beneficial effects on cell migration, growth, and proliferation. The similarity of this hydrogel combination to the extracellular matrix makes it particularly beneficial for tissue regeneration. Crosslinking in a hydrogel has been shown to play an important role in fluid penetration<sup>33</sup> and nutritional support as the size and shape of the pores will greatly affect the movement of these solutes. In this study, we prepared the *in situ* hydrogel on the wound surface through the aldehyde groups of SAD self-crosslinking with the free amino group of CMCTS. Hydrogels prepared *via* self-crosslinking greatly reduce toxicity *in vivo* as they do not involve any additional chemicals. Therefore, the hydrogel used in the present study was not only biocompatible but also biodegradable and induced only a slight

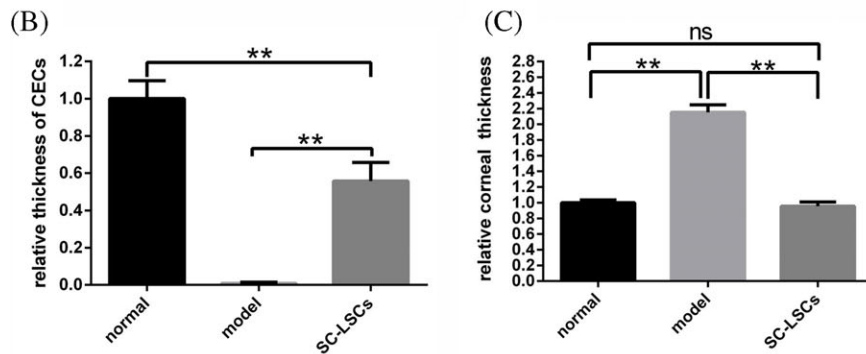
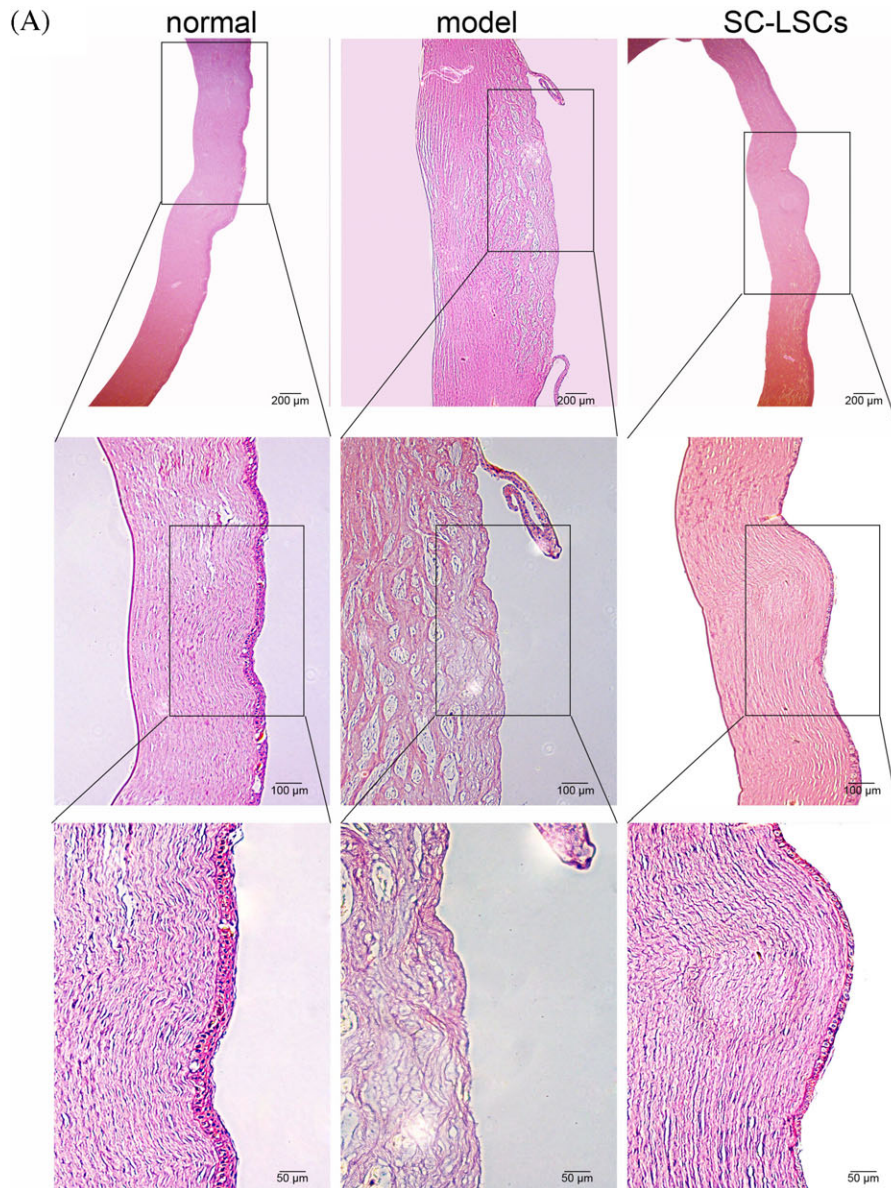


**FIGURE 7.** Treatment with LSC-encapsulated SC hydrogel induces a histological wound healing response in the cornea after alkali burn. (A) Representative images of corneal histology in unburned (normal), untreated alkali burned (model), and hydrogel-treated (SC-LSCs) rabbit corneas 28 days postburn. Scale bars = 200  $\mu\text{m}$  (top panels), 100  $\mu\text{m}$  (middle panels), 50  $\mu\text{m}$  (bottom panels). (B) Relative thickness of CECs compared with normal, model, and hydrogel-treated groups. (C) Total corneal thickness in the normal, model, and hydrogel-treated groups. Data are presented as the mean  $\pm$  SD for each group, \*\* $p < 0.01$ .

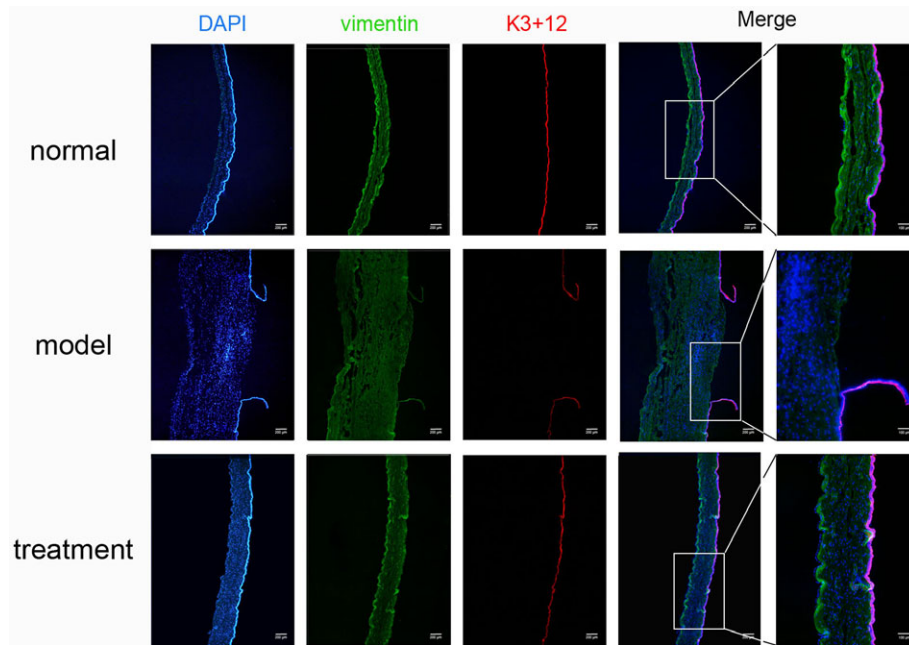


**FIGURE 8.** Treatment with LSC-encapsulated SC hydrogel induces acellular wound healing response in the cornea after alkali burn. K3+12 (red) and vimentin (green) were used as markers of epithelial and stromal cells, respectively, in unburned (normal), untreated alkali burned (model), and hydrogel-treated rabbit corneas. Representative images are shown. Scale bars = 200  $\mu\text{m}$  and 100  $\mu\text{m}$  (right most panels).

inflammatory response immediately after injection, which then decreased over time.

Hydrogel has been shown to prolong the retention time of encapsulated cells effectively which provides a favorable environment for cell migration.<sup>34</sup> In this study, we transplanted LSCs with the *in situ* hydrogel (SC) for repair of corneal tissue following alkali burn injury. The preliminary experimental results showed that the SC prepared in this study could provide a good microenvironment for transplanted cell differentiation and proliferation [Fig. 1(C)]. Besides that, transplanted LSCs can be used to complement the deficient epithelial cells in the wounded tissue and rapidly repair the cornea.<sup>27</sup> LSC-based hydrogels which developed previously required additional surgical manipulation.<sup>35</sup> In the present study, hydrogel-encapsulated LSCs had a rapid effect on the restoration of corneal integrity compared to the untreated corneas after alkali burn. We believe that these effects are largely achieved by the combined use of LSC transplantation and the CMCTS/SAD hydrogel. Previous studies have shown that CMCTS decreases abdominal adhesions and reduces fibrosis,<sup>9,10</sup> which is important for inhibiting scar formation and maintaining epithelial integrity. The corneal keratocytes became over-activated after corneal injury, caused corneal opacity and fibrosis, as well as scar tissue formation.<sup>3</sup> The *in situ* hydrogel produced has good transparency, biocompatibility, and biodegradability and meets the requirements of tissue engineering corneal carrier. But limbal stem cells have good proliferative and differentiation potential, they can supplement the repaired defect epithelial cells. In this study, ACH-encapsulated limbal stem cells were transplanted into the corneal alkali burn site of New Zealand white rabbits. Compared with the model group and the control group, the LSCs survived *in situ* hydrogel

and proliferated and differentiated to some extent. The healing effect on corneal alkali burn wounds is remarkable. In the future research, we will further increase the number and types of samples, and conduct in-depth research on its effects and mechanism of action, providing a potential therapeutic basis for corneal reconstruction based on tissue engineering.

## CONCLUSION

The CMCTS/SAD *in situ* hydrogel prepared in this study was shown to have specific characteristics, including high transparency, high swelling capacity, biocompatibility, and cytocompatibility with LSCs that support its use in tissue engineering applications. The *in situ* hydrogel was proved to transplant encapsulated LSCs to alkali burned corneas successfully, leading to a rapid tissue reconstruction and wound healing. The proposed *in situ* hydrogel could serve as LSCs transplanting scaffold for efficient corneal reconstruction following alkali burn or other types of serious eye injury.

## ACKNOWLEDGMENTS

This study was financially supported by the National Natural Science Foundation of China (81770900, 81401899), the Key Research and Development Program of Shandong Province (2014GHY115025, 2018GSF118197), the Qingdao Science and Technology Plan fund (16-6-2-28-NSH,15-9-1-51-jch), the China Postdoctoral Science Foundation (2017M622144), and the Qingdao Postdoctoral Application Research Project.

## CONFLICT OF INTEREST

The authors declare no financial or commercial conflict of interest.

## REFERENCES

- Singh P, Tyagi M, Kumar Y, Gupta KK, Sharma PD. Ocular chemical injuries and their management. *Oman J Ophthalmol* 2013;6(2): 83–86.
- Bazan HE. Cellular and molecular events in corneal wound healing: Significance of lipid signalling. *Exp Eye Res* 2005;80(4):453–463.
- Chaerkady R, Shao H, Scott SG, Pandey A, Jun AS, Chakravarti S. The keratoconus corneal proteome: Loss of epithelial integrity and stromal degeneration. *J Proteomics* 2013;87:122–131.
- Farid M, Lee N. Ocular surface reconstruction with keratolimbal allograft for the treatment of severe or recurrent symblepharon. *Cornea* 2015;34(6):632–636.
- Ma DH, Chen JK, Zhang F, Lin KY, Yao JY, Yu JS. Regulation of corneal angiogenesis in limbal stem cell deficiency. *Prog Retin Eye Res* 2006;25(6):563–590.
- Xiang J, Sun JG, Hong JX, Wang WT, Wei AJ, Le QH, Xu JJ. T-style keratoprosthesis based on surface-modified poly (2-hydroxyethyl methacrylate) hydrogel for cornea repairs. *Mater Sci Eng C-Mater Biological App* 2015;50:274–285.
- Fonseca-Santos B, Chorilli M. An overview of carboxymethyl derivatives of chitosan: Their use as biomaterials and drug delivery systems. *Mater Sci Eng C-Mater Biological App* 2017;77:1349–1362.
- Nascimento AV, Singh A, Bousbaa H, Ferreira D, Sarmento B, Amiji MM. Mad2 checkpoint gene silencing using epidermal growth factor receptor-targeted chitosan nanoparticles in non-small cell lung cancer model. *Mol Pharm* 2014;11(10):3515–3527.
- Ren C, Zhao D, Zhu L. Use of N,O-carboxymethyl chitosan to prevent postsurgical adhesions in a rabbit double uterine horn model: A randomized controlled design. *Sci China Life Sci* 2016;59(5):504–509.
- Li XD, Xia DL, Shen LL, He H, Chen C, Wang YF, Chen YP, Guo LY, Gu HY. Effect of "phase change" complex on postoperative adhesion prevention. *J Surg Res* 2016;202(1):216–224.
- Ito T, Yeo Y, Highley CB, Bellas E, Benitez CA, Kohane DS. The prevention of peritoneal adhesions by in situ cross-linking hydrogels of hyaluronic acid and cellulose derivatives. *Biomaterials* 2007;28(6): 975–983.
- Maia J, Ferreira L, Carvalho R, Ramos MA, Gil MH. Synthesis and characterization of new injectable and degradable dextran-based hydrogels. *Polymer* 2005;46(23):9604–9614.
- Nishi KK, Jayakrishnan A. Preparation and in vitro evaluation of primaquine-conjugated gum arabic microspheres. *Biomacromolecules* 2004;5(4):1489–1495.
- Ruhela D, Riviere K, Szoka FC. Efficient synthesis of an aldehyde functionalized hyaluronic acid and its application in the preparation of hyaluronan-lipid conjugates. *Bioconjug Chem* 2006;17(5):1360–1363.
- Wang DA, Varghese S, Sharma B, Strehin I, Fermanian S, Gorham J, Fairbrother DH, Cascio B, Elisseff JH. Multifunctional chondroitin sulphate for cartilage tissue-biomaterial integration. *Nat Mater* 2007;6(5):385–392.
- Dauil P, Feraille L, Elena PP, Garrigue JS. Comparison of the anti-inflammatory effects of artificial tears in a rat model of corneal scraping. *J Ocul Pharmacol Ther* 2016;32(2):109–118.
- Balakrishnan B, Jayakrishnan A. Self-cross-linking biopolymers as injectable in situ forming biodegradable scaffolds. *Biomaterials* 2005; 26(18):3941–3951.
- Chen J, Li S, Zhang Y, Wang W, Zhang X, Zhao Y, Wang Y, Bi H. A reloadable self-healing hydrogel enabling diffusive transport of C-dots across gel-gel interface for scavenging reactive oxygen species. *Adv Healthc Mater* 2017;6(21):1–10.
- Xu Y, Han J, Lin H. Fabrication and characterization of a self-crosslinking chitosan hydrogel under mild conditions without the use of strong bases. *Carbohydr Polym* 2017;156:372–379.
- Liang Y, Liu W, Han B, Yang C, Ma Q, Song F, Bi Q. An in situ formed biodegradable hydrogel for reconstruction of the corneal endothelium. *Colloids Surf B Biointerfaces* 2011;82(1):1–7.
- Xu W, Wang Z, Liu Y, Wang L, Jiang Z, Li T, Zhang W, Liang Y. Carboxymethyl chitosan/gelatin/hyaluronic acid blended-membranes as epithelia transplanting scaffold for corneal wound healing. *Carbohydr Polym* 2018;192:240–250.
- Ashri A, Amalina N, Kamil A, Fazry S, Sairi MF, Nazar MF, Lazim AM. Modified *Dioscorea hispida* starch-based hydrogels and their in-vitro cytotoxicity study on small intestine cell line (FHS-74 Int). *Int J Biol Macromol* 2018;107:2412–2421.
- Li YJ, Yang YL, Yang L, Zeng YX, Gao XW, Xu HW. Poly(ethylene glycol)-modified silk fibroin membrane as a carrier for limbal epithelial stem cell transplantation in a rabbit LSCD model. *Stem Cell Res Therapy* 2017;8(1):256.
- Hu TZ, Fei ZH, Wei N. Chemosensitive effects of Astragaloside IV in osteosarcoma cells via induction of apoptosis and regulation of caspase-dependent Fas/FasL signaling. *Pharmacol Rep* 2017;69(6):1159–1164.
- Liang Y, Xu W, Han B, Li N, Zhao W, Liu W. Tissue-engineered membrane based on chitosan for repair of mechanically damaged corneal epithelium. *J Mater Sci Mater Med* 2014;25(9):2163–2171.
- Cotsarelis G, Cheng SZ, Dong G, Sun TT, Lavker RM. Existence of slow-cycling limbal epithelial basal cells that can be preferentially stimulated to proliferate: Implications on epithelial stem cells. *Cell* 1989;57(2):201–209.
- Yazdanpanah G, Jabbehdari S, Djalilian AR. Limbal and corneal epithelial homeostasis. *Curr Opin Ophthalmol* 2017;28(4):348–354.
- Zoega GM, Kristinsson JK. Chemical injuries of the eye—management of alkali burns. *Laeknabladid* 2004;90(6):491–493.
- Yao L, Li ZR, Su WR, Li YP, Lin ML, Zhang WX, Liu Y, Wan Q, Liang D. Role of mesenchymal stem cells on cornea wound healing induced by acute alkali burn. *PLoS One* 2012;7(2):e30842.
- Dua HS. The conjunctiva in corneal epithelial wound healing. *Br J Ophthalmol* 1998;82(12):1407–1411.
- Tsai CY, Woung LC, Yen JC, Tseng PC, Chiou SH, Sung YJ, Liu KT, Cheng YH. Thermosensitive chitosan-based hydrogels for sustained release of ferulic acid on corneal wound healing. *Carbohydr Polym* 2016;135:308–315.
- Synowiecki J, Al-Khateeb NA. Production, properties, and some new applications of chitin and its derivatives. *Crit Rev Food Sci Nutr* 2003;43(2):145–171.
- Speer DP, Chvapil M, Eskelson CD, Ulreich J. Biological effects of residual glutaraldehyde in glutaraldehyde-tanned collagen biomaterials. *J Biomed Mater Res* 1980;14(6):753–764.
- Gratieri T, Gelfuso GM, Rocha EM, Sarmento VH, de Freitas O, Lopez RFV. A poloxamer/chitosan in situ forming gel with prolonged retention time for ocular delivery. *Eur J Pharm Biopharm* 2010;75(2):186–193.
- Chen D, Qu Y, Hua X, Zhang L, Liu Z, Pflugfelder SC, Li DQ. A hyaluronan hydrogel scaffold-based xeno-free culture system for ex vivo expansion of human corneal epithelial stem cells. *Eye* 2017; 31(6):962–971.